SCIENTIFIC REPORTS

OPEN

SUBJECT AREAS:
COMPUTER SCIENCE
COMPLEX NETWORKS
APPLIED MATHEMATICS
CHEMICAL PHYSICS

Received
29 October 2014

Accepted
12 February 2015

Published
12 March 2015

Correspondence and requests for materials should be addressed to Z.Z.Z. (zhangzz@fudan.edu.cn)

Laplacian spectra of a class of small-world networks and their applications

Hongxiao Liu[1,2], Maxim Dolgushev[3], Yi Qi[1,2] & Zhongzhi Zhang[1,2]

[1]School of Computer Science, Fudan University, Shanghai 200433, China, [2]Shanghai Key Laboratory of Intelligent Information Processing, Fudan University, Shanghai 200433, China, [3]Theoretical Polymer Physics, University of Freiburg, Hermann-Herder-Str.3, D-79104 Freiburg, Germany.

One of the most crucial domains of interdisciplinary research is the relationship between the dynamics and structural characteristics. In this paper, we introduce a family of small-world networks, parameterized through a variable d controlling the scale of graph completeness or of network clustering. We study the Laplacian eigenvalues of these networks, which are determined through analytic recursive equations. This allows us to analyze the spectra in depth and to determine the corresponding spectral dimension. Based on these results, we consider the networks in the framework of generalized Gaussian structures, whose physical behavior is exemplified on the relaxation dynamics and on the fluorescence depolarization under quasiresonant energy transfer. Although the networks have the same number of nodes (beads) and edges (springs) as the dual Sierpinski gaskets, they display rather different dynamic behavior.

One of the most major problems in the study of networks is to understand the relations between their topology and the dynamics[1]. For instance, in the framework of generalized Gaussian structures (GGSs)[2–5], the dynamics of polymer networks is fully described through the Laplacian eigenvectors and eigenvalues. In the field of GGSs and dynamical processes, the investigation of Laplacian eigenmodes has a paramount importance for the relaxation dynamics, the fluorescence depolarization by quasiresonant energy transfer[6–8], the mean first-passage time problems[9–11], and so on. Laplacian eigenvalues and eigenvectors play an irreplaceable role and they are also relevant to multi-aspects of complex network structures, like spanning trees[12], resistance distance[13] and community structure[14]. However, it is a challenging task to derive exact Laplacian eigenvalues or eigenvectors for a complex system and based on them to describe its dynamics. We remark that for this the use of deterministic structures is of much help[15–19]. Although the structural disorder leads in case of many real networks like hyperbranched polymers to smoothing-out and averaging, the topological features are still reflected in the typical scaling behaviors[20]. Furthermore, recently a striking development of chemistry made possible the synthesis of the hierarchical, fractal Sierpinski-type compounds[21]. Undoubtedly, this new achievement will keep the interest of the theorists on the regular structures, especially on those with loops.

The study of Laplacian eigenvalues has exhibited its activity during the past few decades, among extensive subjects and researches. The works from last century had solved the Laplacian eigenvalues for considerable amount of famous networks, like dual Sierpinski gaskets (in 2 or higher dimensions)[15,16], dendrimers[17], and Vicsek fractals[18,19]. Another type of model structures, which often arise in the complex systems or polymer networks, are the so-called small-world networks (SWNs)[22–25]. Recent studies have also suggested that SWNs play a notable role in real life[26,27].

In this report we introduce a new kind of SWNs. Their construction is based on complete graphs consisting of d nodes and they have the same number of nodes and of edges as the dual Sierpinski gaskets embedded in $(d-1)$-dimension. A complete graph is a simple undirected graph in which every pair of distinct vertices is connected by a unique edge. It has been widely used in quantum walks[28,29], tensor networks[30], social networks[31], and explosive percolation problem[32]. While the SWNs introduced here are based on complete graph, their clustering coefficient shows that the SWNs are similar to complete graphs only in the limit $d \to \infty$. As we proceed to show, also in this limit they have similar behavior as the dual Sierpinski gaskets embedded in to $d \to \infty$ dimensions. On the other hand, for finite d, the SWNs display a macroscopically distinguishable behavior.

The report is organized as follows: First, we present the construction of SWNs, analyze their properties and their Laplacian spectra (the derivation of the recursive equations for the eigenvalues is given in Methods). Then,

based on the spectra we consider the dynamics of networks, namely, the structural average of the mean monomer displacement under applied constant force and the mechanical relaxation moduli, and the dynamics on networks, exemplified through the fluorescence depolarization. Finally, we summarize and discuss our results.

Results

Model structures. We start with a brief introduction to a family of small-world networks (SWNs) Ω_g^d characterized by two parameters d and g, where d stands for the number of nodes of complete graph and g for the current generation. Figure 1 shows a construction process from Ω_1^3 to Ω_3^3: At first, Ω_1^3 is a simple triangle, that is, a complete graph with 3 nodes. At the next stage, each node in Ω_1^3 is replaced by a new complete graph. Thus each of the newly appeared complete graphs contains exactly one node of Ω_1^3 and we get the network at second generation Ω_2^3. The growth process to the next generation continues in a similar way: Connecting a complete graph to each of the node of Ω_2^3 one gets Ω_3^3. In general, we have d^{g-1} nodes at generation $g-1$. By attaching $d-1$ nodes to each existing node, increases their total number from d^{g-1} to d^g. In this way, we get immediately the number of nodes in this network, $N_g^d = d^g$, and the number of edges, $E_g^d = \frac{1}{2}\left(d^{g+1}-d\right)$. It has to be mentioned that the dual Sierpinski gaskets embedded in $(d-1)$-dimension have exactly the same number of nodes and of edges[33].

To give evidence of the small-world property, we consider another characteristics, the diameter of the network. For a network, the diameter means the maximum of the shortest distances between all pairs of nodes in it[1]. Let $D\left(\Omega_g^d\right)$ be the diameter of network Ω_g^d. It is clearly that at generation $g = 1$, $D(\Omega_1^d) = 1$. At each iteration $g \geq 1$, new complete graphs are added to each vertex. Let us define the two nodes with longest distance in the existing network as M_A and M_B. It is easy to see that these two nodes belong to the complete graphs attached to M_A and M_B, respectively. Hence, at any iteration, the diameter of the network increases by 2 at most. Then the diameter of Ω_g is just equal to $2g-1$, a result irrelevant to parameter d. The value can be presented by another form $2\log_d N_g - 1$, which grows logarithmically with the network size indicating that the networks Ω_g^d are small-world[1].

Now we turn to the clustering coefficient of any node i, which is given by $C_i = 2e_i/[k_i(k_i-1)]$, where e_i is the number of existing links between all the k_i neighbors of node i[34]. From the network construction, we come to a simple conclusion that if node x exists for h generations, external $(d-1)h$ nodes will be attached to it. That is, $k_x = (d-1)h$. Among the $(d-1)h$ neighbors, $d-1$ nodes that belong to the same complete graph are connected to each other, leading to the total number of links $e_x = h[(d-1)(d-2)/2]$. Thus, the C_x is given by

$$C_x = \frac{2e_x}{k_x(k_x-1)} = \frac{d-2}{h(d-1)-1}. \quad (1)$$

Based on equation (1) we can list the correspondence between each kind of clustering coefficient and the corresponding amount of nodes:

$$C_i = \begin{cases} 1 & \text{for } (d-1)d^{g-1} \text{ nodes,} \\ \dfrac{d-2}{2(d-1)-1} & \text{for } (d-1)d^{g-2} \text{ nodes,} \\ \vdots & \vdots \\ \dfrac{d-2}{g(d-1)-1} & \text{for } (d-1)d^{0}+1 \text{ nodes,} \end{cases} \quad (2)$$

where the last situation represents the center of the whole network. Then we can obtain the average clustering coefficient of all the nodes,

$$\langle C\rangle = \frac{1}{N_g^d}\left[\frac{d-2}{(d-1)g-1} + \sum_{k=1}^{g}(d-1)d^{g-k}\frac{d-2}{(d-1)k-1}\right]. \quad (3)$$

Figure 2 shows $\langle C\rangle$ as a function of g for d going from 3 to 6. As one can infer from the figure, $\langle C\rangle$ decreases very rapidly at small generations to a some constant value, which depends on d. In fact, one can find from equation (3) that for Ω_∞^d the average clustering coefficient is given by $\langle C\rangle_\infty(d) = ((d-1)/d)_2F_1[(d-2)/(d-1), 1; (2d-3)/(d-1); 1/d]$, where ${}_2F_1[\ldots]$ is the hypergeometric function, i.e. $\langle C\rangle_\infty(3) \approx 0.76$, $\langle C\rangle_\infty(4) \approx 0.84$, $\langle C\rangle_\infty(5) \approx 0.88$, and $\langle C\rangle_\infty(6) \approx 0.9$. For very large d ($d \to \infty$), equation (3) converges to value $\bar{C} = 1$, an inherent property of a complete graph.

Recursion formulae for the Laplacian spectrum. Let $\mathbf{A}_g^d = [A_{ij}]_{d^g \times d^g}$ denote the adjacency matrix of Ω_g^d, where $A_{ij} = A_{ji} = 1$ if nodes i and j are adjacent, $A_{ij} = A_{ji} = 0$ otherwise, then the degree of node i is $d_i = \sum_{j\in\Omega_g^d} A_{ij}$. Let $\mathbf{D}_g^d = \mathrm{diag}(d_1, d_2, \ldots, d_{d^g})$ denote the diagonal degree matrix of Ω_g^d, then the Laplacian matrix of Ω_g^d is defined by $\mathbf{L}_g^d = \mathbf{D}_g^d - \mathbf{A}_g^d$.

To get a solution for the eigenvalues of $\mathbf{L}\left(\Omega_g^d\right)$, we have to concentrate our attention on its characteristic polynomial, $P_g^d(\lambda)$. Here we just give a result and put off the proof and details in Methods:

$$\begin{aligned} P_g^d(\lambda) &= \det\left(\lambda\mathbf{I} - \mathbf{L}\left(\Omega_g^d\right)\right) \\ &= (\lambda-1)^{d^{g-1}}(\lambda-d)^{(d-2)d^{g-1}} P_{g-1}^d\left(\frac{\lambda(\lambda-d)}{\lambda-1}\right). \end{aligned} \quad (4)$$

The recursion relation provided in equation (4) determines the eigenvalues of Laplacian matrix for Ω_g^d. Note that P_g^d has a factor

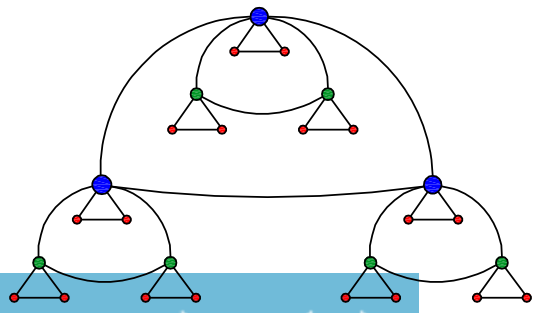

Figure 1 | Construction of Ω_g^d for $d = 3$ and $g = 1$ (blue beads), $g = 2$ (blue and green beads), $g = 3$ (all beads).

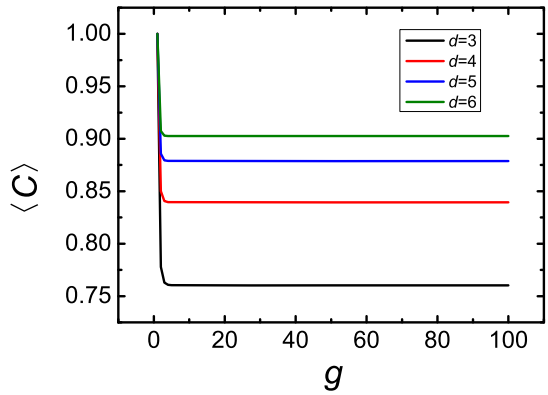

Figure 2 | Clustering coefficients of Ω_g^d for the parameters d from 3 to 6, when g varies from 1 to 100.

$\lambda - d$ with exponent $(d-2)d^{g-1}$, i.e. equation (4) has the root $\lambda = d$ with multiplicity at least $(d-2)d^{g-1}$.

It is evident that Ω_g^d has d^g Laplacian eigenvalues, denoted by λ_1^g, λ_2^g, …, $\lambda_{d^g}^g$, the set of which is represented by Λ_g, i.e., $\Lambda_g = \{\lambda_1^g, \lambda_2^g, \ldots, \lambda_{d^g}^g\}$. In addition, without loss of generality, we assume that $\lambda_1^g \le \lambda_2^g \le \ldots \le \lambda_{d^g}^g$. On the basis of above analysis, Λ_g can be divided into two subsets $\Lambda_g^{(1)}$ and $\Lambda_g^{(2)}$ satisfying $\Lambda_g = \Lambda_g^{(1)} \cup \Lambda_g^{(2)}$, where $\Lambda_g^{(1)}$ contains all eigenvalues equal to d, while $\Lambda_g^{(2)}$ includes the remaining eigenvalues. Thus,

$$\Lambda_g^{(1)} = \underbrace{\{d, d, d, \ldots, d, d\}}_{d^g - 2\,d^{g-1}}. \tag{5}$$

The remaining $2d^{g-1}$ eigenvalues belonging to $\Lambda_g^{(2)}$ are determined by $(\lambda-1)^{d^{g-1}} P_{g-1}^d\left(\frac{\lambda(\lambda-d)}{\lambda-1}\right) = 0$. Let the $2d^{g-1}$ eigenvalues be $\tilde{\lambda}_1^g$, $\tilde{\lambda}_2^g$, …, $\tilde{\lambda}_{2d^{g-1}}^g$, respectively. That is, $\Lambda_g^{(2)} = \left\{\tilde{\lambda}_1^g, \tilde{\lambda}_2^g, \ldots, \tilde{\lambda}_{2d^{g-1}}^g\right\}$. Given that the P_{g-1}^d is the characteristic polynomial of $\mathbf{L}\left(\Omega_{g-1}^d\right)$ leading to N_{g-1} eigenvalues $\Lambda_{g-1} = \left\{\lambda_1^{g-1}, \lambda_2^{g-1}, \ldots, \lambda_{d^{g-1}}^{g-1}\right\}$, the set $\Lambda_g^{(2)}$ follows from

$$\prod_{i=1}^{d^{g-1}} \left(\lambda(\lambda-d) - \lambda_i^{g-1}(\lambda-1)\right) = 0 \tag{6}$$

or from

$$\lambda^2 - \left(\lambda_i^{g-1} + d\right)\lambda + \lambda_i^{g-1} = 0, \tag{7}$$

where i runs from 1 to $N_{g-1} = d^{g-1}$.

Solving the quadratic equation (7), we obtain two roots $\tilde{\lambda}_i^g = r_1\left(\lambda_i^{g-1}\right)$ and $\tilde{\lambda}_{i+d^{g-1}}^g = r_2\left(\lambda_i^{g-1}\right)$, where $r_1(x)$ and $r_2(x)$ are

$$r_1(x) = \frac{1}{2}\left(d + x - \sqrt{d^2 + 2dx + x^2 - 4x}\right) \tag{8}$$

and

$$r_2(x) = \frac{1}{2}\left(d + x + \sqrt{d^2 + 2dx + x^2 - 4x}\right), \tag{9}$$

respectively. Thus, each eigenvalue λ_i^{g-1} of Λ_{g-1} gives rise to two new eigenvalues in $\Lambda_g^{(2)}$ by inserting each Laplacian eigenvalue of Ω_{g-1} into equations (8) and (9). Considering the initial value $E_1 = \{0, \underbrace{d, d, d, \ldots, d, d}_{d-1}\}$, by recursively applying equations (8) and (9) and accounting for $\Lambda_g^{(1)}$, the Laplacian eigenvalues of Ω_g are fully determined.

It is simple matter to check that equations (8) and (9) have the following behaviors:

$$r_1(x) \simeq \begin{cases} x/d & \text{for } 0 \le x \ll 1, \\ 1 - \dfrac{d-1}{x} & \text{for } x \gg d \end{cases} \tag{10}$$

and

$$r_2(x) \simeq \begin{cases} d + \dfrac{d-1}{d}x & \text{for } 0 \le x \ll 1, \\ x & \text{for } x \gg d. \end{cases} \tag{11}$$

In this way equation (10) produces only small eigenvalues, $r_1(x) \in [0, 1)$ and equation (11) the large ones, $r_2(x) \in [d, \infty)$. Thus, the eigenvalue spectrum has always a gap $[1, d)$, which is bigger for networks Ω_g^d with larger d.

Now, it is interesting to examine the behavior of the small eigenvalues, i.e. to consider equation (10) for $0 \le x \ll 1$. Our goal is to obtain the spectral dimension $\tilde{d}$ (also known as fracton dimension[35]). For this we use the methods of Ref. 36. Under equation (10) for $x \ll 1$, the n eigenvalues in the interval $[\lambda^g, \lambda^g + \Delta\lambda^g]$ go over in n eigenvalues in the interval $[\lambda^{g+1}, \lambda^{g+1} + \Delta\lambda^{g+1}/d]$, while the total number of modes increases from N to dN. Hence, the density of states (modes) $\rho(\lambda)$ for $\lambda \ll 1$ obeys

$$N\rho(\lambda)\Delta\lambda = dN\rho(\lambda/d)\Delta\lambda/d, \quad \text{i.e. } \rho(\lambda) = \rho(\lambda/d). \tag{12}$$

Using now the relation between $\rho(\lambda)$ and the spectral dimension $\tilde{d}$[35],

$$\rho(\lambda) \sim \lambda^{\tilde{d}/2-1} \tag{13}$$

leads to

$$d^{\tilde{d}/2-1} = 1. \tag{14}$$

This means that the spectral dimension of the networks Ω_g^d is $\tilde{d} = 2$ and $\tilde{d}$ is independent on d. We note that for the dual Sierpinski gasket embedded in $(d-1)$-dimension the spectral dimension is $\tilde{d} = 2\ln(d)/\ln(d+2)$, see e.g. Refs. 37, 38, i.e. it is similar to that of Ω_g^d only in the limit $d \to \infty$.

Dynamics of polymer networks under external forces. We are going to study the networks Ω_g^d under the framework of generalized Gaussian structures (GGS)[3–5], an extension of the classical Rouse beads-springs model[2,39–41]. Here we let all N beads of the GGS to be assigned to the same friction constant, ζ. The beads are connected to each other by elastic springs with spring constant K. The Langevin equation of motion for the mth bead in a system reads

$$\zeta\frac{d\mathbf{R}_m(t)}{dt} + K\sum_{i=1}^{N} L_{mi}\mathbf{R}_i(t) = \mathbf{f}_m(t) + \mathbf{F}_m(t), \tag{15}$$

where $\mathbf{R}_m(t) = (X_m(t), Y_m(t), Z_m(t))$ is the position vector of the mth bead at time t, $\mathbf{L}$ describing the Laplacian matrix of the Ω_g^d. Moreover, $\mathbf{f}_m(t)$ is the thermal noise that is assumed to be Gaussian with zero mean value $\langle \mathbf{f}_m(t)\rangle = 0$ and $\langle f_{m\alpha}(t) f_{n\beta}(t')\rangle = 2k_B T\delta_{\alpha\beta}\delta_{\mathrm{mn}}\delta(t-t')$, where k_B is the Boltzmann constant, T is the temperature, α and β represent the x, y, and z directions; $\mathbf{F}_m(t)$ is the external force acting on bead m.

First, we consider a quantity which is related to the micromanipulations with the polymer networks[42]. We put a constant external force $\mathbf{F}_k(t) = F\Theta(t)\delta_{mk}\mathbf{e}_y$ ($\forall k$), started to act at $t = 0$ ($\Theta(t)$ is the Heaviside step function) on a single bead m of the Ω_g^d in the y direction. After averaging over all possibilities of choosing this monomer randomly, the displacement reads[4,5,39]

$$\langle Y(t)\rangle = \frac{Ft}{N\zeta} + \frac{F}{\sigma N\zeta}\sum_{i=2}^{N}\frac{1-\exp(-\sigma\lambda_i t)}{\lambda_i}, \tag{16}$$

where $\sigma = K/\zeta$ is the bond rate constant, and λ_i is the eigenvalues of matrix $\mathbf{L}$ with λ_1 being the unique smallest eigenvalue 0.

Another example is the response to harmonically applied forces (strain fields), i.e. $\mathbf{F}_m(t) = \gamma_0 e^{i\omega t} Y_m(t)\mathbf{e}_x$. The related response function is the so-called complex dynamic modulus $G^*(\omega)$, or equivalently, its real $G'(\omega)$ and imaginary $G''(\omega)$ components (the storage and the loss moduli[41,43]). In the GGS model (for very dilute theta-solutions) the $G'(\omega)$ and $G''(\omega)$ are given by[3]

$$G'(\omega) = \frac{\nu k_B T}{N}\sum_{i=2}^{N}\frac{(\omega/2\sigma\lambda_i)^2}{1+(\omega/2\sigma\lambda_i)^2} \tag{17}$$

and

$$G''(\omega)=\frac{vk_BT}{N}\sum_{i=2}^{N}\frac{\omega/2\sigma\lambda_i}{1+(\omega/2\sigma\lambda_i)^2}, \tag{18}$$

where v denotes the number of polymer segments (beads) per unit volume.

We start by focusing on the averaged displacement $\langle Y(t)\rangle$, equation (16), where we set $\sigma = 1$ and $\frac{F}{\zeta}=1$. Figure 3 displays in double logarithmic scales the $\langle Y(t)\rangle$ for the networks Ω_g^4 consisting of 4^7 up to 4^{10} beads. As is known[4,5,39], the $\langle Y(t)\rangle$ in such GGS at very long times reaches the domain $\langle Y(t)\rangle \sim Ft/(N\zeta)$ and at very short times obeying $\langle Y(t)\rangle \sim Ft/\zeta$. However, in intermediate regime the network's beads move for several decades of time very slowly (logarithmic behavior[5]), up to the times $t \sim N$ related to the diffusive motion of the whole structure. This differs from the corresponding patterns for the dual Sierpinski gaskets (embedded in $(d-1)$-dimension)[37,38], which show a slow subdiffusive behavior $\langle Y(t)\rangle \sim t^{\alpha}$ with $\alpha \approx 0.23$ for $d = 4$.

While the $\langle Y(t)\rangle$ of Ω_g^d do not scale in the intermediate domain, the mechanical relaxation functions show in the related frequency domain a scaling behavior, see the results for storage moduli $G'(\omega)$ presented in Fig. 4. Here we plot them in dimensionless units by setting $\sigma = 1$ and $\frac{vk_BT}{N}=1$. The networks are the same as for $\langle Y(t)\rangle$ of Fig. 3. The $G'(\omega)$ behaves commonly at very small and very high frequencies as ω^2 and ω^0, respectively. The in-between region of $G'(\omega)$ (related to the intermediate time domain of $\langle Y(t)\rangle$) the curves give in double-logarithmic scales the slopes around 1. This result is bigger than that in the same region of the corresponding dual Sierpinski gaskets embedded into 3-dimensional space (there one has slopes near 0.77)[37]. For a better visualization, we plot in the inset of Fig. 4 the effective slopes $\alpha'=\frac{d(\log_{10}G')}{d(\log_{10}\omega)}$ for the same curves of Fig. 4. As expected, the limiting behaviors for very low and very high frequencies hold for slope 2 and slope 0. But in the intermediate frequency region, all of the four curves become wavy. Such a waviness reflects typically[36–38] a very symmetric, hierarchical character of the structures. In case of real polymer systems, the inherit structural disorder smooths out such wavy patterns, while keeping the characteristic intermediate scaling[20]. Finally, the curves cross each other at the slope 1, keeping a short stable period and then falling into a value of 0.5.

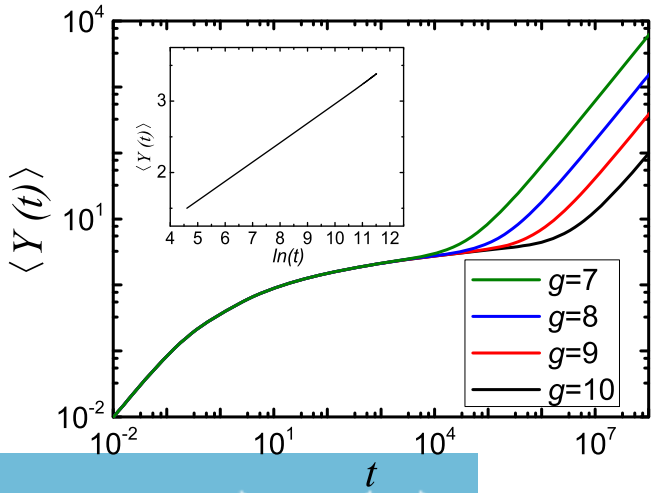

Figure 3 | Averaged monomer displacement $\langle Y(t)\rangle$ for Ω_g^4, where g runs from 7 to 10.

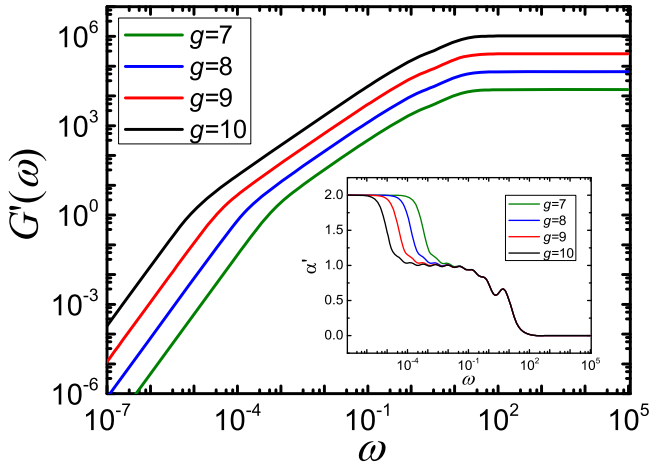

Figure 4 | Storage modulus $G'(\omega)$ for Ω_g^4, where g runs from 7 to 10.

Fluorescence depolarization. We are now embarking on the dynamics of energy transfer over a system of chromophores[6–8]. As a usual way, we assume that the nodes (beads) only transfer their energy with their nearest neighbors. Under these conditions the dipolar quasiresonant energy transfer among the chromophores obeys the following equation[6–8]:

$$\frac{dP_i(t)}{dt}=\sum_{\substack{j=1\\ j\neq 1}}^{N_g}T_{ij}P_j(t)-\left(\sum_{\substack{j=1\\ j\neq i}}^{N_g}T_{ij}\right)P_i(t), \tag{19}$$

where $P_i(t)$ represents the probability that node i is excited at time t and T_{ij} is the transfer rate from node j to node i. Following the framework of Refs. 6–8, we separate the radiative decay (equal for all chromophores) from the transfer problem, which can be included by the multiplication of all the $P_i(t)$ by $\exp(-t/\tau_R)$, where $1/\tau_R$ corresponding to the radiative decay rate. Under the assumption that all microscopic rates are equal to each other, fixed on a value $\tilde{k}$, equation (19) becomes

$$\frac{dP_i(t)}{dt}=-\tilde{k}\sum_{\substack{j=1\\ j\neq 1}}^{N_g}L_{ij}P_j(t)-\left(\tilde{k}L_{ii}\right)P_i(t), \tag{20}$$

where L_{ij} is the ijth entry of Laplacian matrix $\mathbf{L}_g$. In equation (20) we used that for $\mathbf{L}_g$ the relation $L_{ii}=-\sum_{j\neq i}L_{ji}$ holds.

The solution of equation (20) requires diagonalization of $\mathbf{L}_g$. The result for a given $P_i(t)$ depends both on the eigenvalues and on the eigenvectors of $\mathbf{L}_g$[6–8]. However, by averaging over all sites (a procedure fully justified when the dipolar orientations are independent of the beads' position in the system), the probability of finding the excitation at time t on the originally excited chromophore depends only on the eigenvalues of $\mathbf{L}_g$ and is given by[6–8]

$$\langle P(t)\rangle=\frac{1}{N_g}\sum_{i=1}^{N_g}\exp\left(-\tilde{k}\lambda_i^g t\right). \tag{21}$$

Measuring the time in units of $1/\tilde{k}$, we can obtain the $\langle P(t)\rangle$ with $\tilde{k}=1$. In Fig. 5 we display in double logarithmic scales the average probability $\langle P(t)\rangle$ that an initially excited chromophore of the network Ω_g^d is still or again excited at time t. As for the previous figures, we choose $d = 4$ and change the generation g from 7 to 10, which means that the number of beads varies from 4^7 to 4^{10}. From Fig. 5 a waviness superimposed at early times can be observed immediately. Such waviness has been predicted in the regular hyperbranched

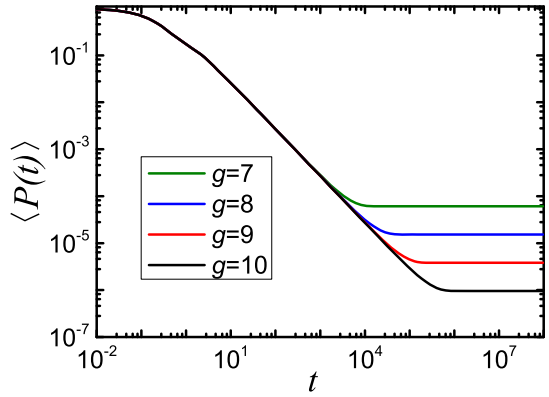

Figure 5 | The average probability $\langle P(t)\rangle$, equation (21), for Ω_g^4, where g runs from 7 to 10.

fractals[6] and it is related to high symmetry (regularity) of the network, i.e. the averaging due to possible disorder will smooth out the curves. Besides, in the intermediate time domain the decays show a power-law behavior, i.e. $\langle P(t)\rangle \sim t^{-\alpha}$. In Fig. 5 the α float around 0.98 for all four generations, a very high value among similar kinds of networks.

For the sake of comparison, in Fig. 6 we display the $\langle P(t)\rangle$ for dual Sierpinski gaskets embedded into 3-dimensional space for generations g as those in Fig. 5. What is clear from the figure, the curves also scale in the intermediate time domain, but have a smaller scaling exponent $\alpha = 0.78$ compared to that of the networks introduced in this paper. Moreover, the four curves saturate to a constant value later than those of Fig. 5, while the plateau values $\langle P(\infty)\rangle$ are exactly the same for both figures and equal to $1/N_g$[6,7]. This indicates that the equipartition of the energy over all beads is reached faster for the Ω_g^d networks than for the dual Sierpinski gaskets with the same number of nodes and edges.

Discussion

In summary, we have introduced a class of small-world networks constructed based on complete graphs. First, we have calculated the full Laplacian spectrum obtained from recursion formulae and proved its completeness. The corresponding analytic expressions allowed us to analyze the eigenvalues in detail and to calculate the related spectral dimension $\tilde{d}$. Using the eigenvalues, we have discussed the dynamics of such polymer networks in the GGSs framework, as well as the energy transfer through fluorescence depolarization. The ensuing spectral dimension $\tilde{d} = 2$ leaves its fingerprints in all quantities considered in the paper. In the intermediate time or frequency domain they follow the asymptotic relations[5–7,35,36]:

$$\langle Y(t)\rangle \sim \ln t, \tag{22}$$

$$G'(\omega) \sim G''(\omega) \sim \omega^{\tilde{d}/2} = \omega^1, \tag{23}$$

$$\langle P(t)\rangle \sim t^{-\tilde{d}/2} = t^{-1}, \tag{24}$$

which were proven here by the numerical calculations. The networks introduced here are deterministic and highly structured, however, in case of a possible weak disorder leading to smoothing out of the curves the conclusions will still hold.

We believe that recent advances in the synthesis of fractal supramacromolecular polymers[21] will open new perspectives for the compounds constructed based on the symmetric small-world networks presented in the report. Finally, we remark that we expect to find more applications of the networks considered here; in particular, the analytic expressions for the Laplacian eigenvalues determined here will be of much help.

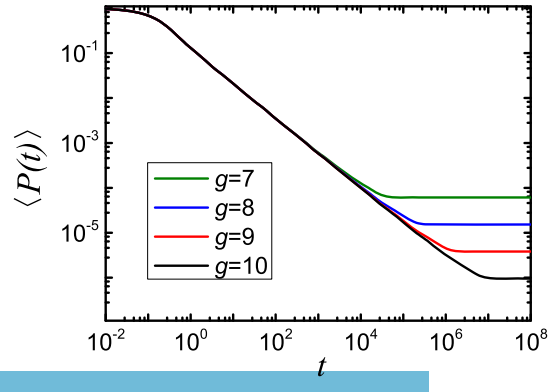

Figure 6 | The average probability $\langle P(t)\rangle$, corresponding to the dual Sierpinski gaskets embedded into 3-dimension. The generation g runs from 7 to 10.

Methods

Characteristic polynomial for the Laplacian eigenvalues of Ω_g^d. Following from the construction of Ω_g^d, the adjacency matrix $\mathbf{A}\left(\Omega_g^d\right)$, the degree matrix $\mathbf{D}\left(\Omega_g^d\right)$, and the Laplacian matrix $\mathbf{L}\left(\Omega_g^d\right)$ can be expressed as

$$\mathbf{A}\left(\Omega_g^d\right) = \begin{pmatrix} \mathbf{A}\left(\Omega_{g-1}^d\right) & \mathbf{I} & \mathbf{I} & \cdots & \mathbf{I} \\ \mathbf{I} & 0 & \mathbf{I} & \cdots & \mathbf{I} \\ \mathbf{I} & \mathbf{I} & 0 & \cdots & \mathbf{I} \\ \vdots & \vdots & \vdots & \ddots & \vdots \\ \mathbf{I} & \mathbf{I} & \mathbf{I} & \cdots & 0 \end{pmatrix}_{d\times d} \tag{25}$$

$$\mathbf{D}\left(\Omega_g^d\right) = \mathrm{diag}\left(\mathbf{D}\left(\Omega_{g-1}^d\right) + (d-1)\mathbf{I}, (d-1)\mathbf{I}, \cdots, (d-1)\mathbf{I}\right)_{d\times d'} \tag{26}$$

and

$$\mathbf{L}\left(\Omega_g^d\right) = \mathbf{D}\left(\Omega_g^d\right) - \mathbf{A}\left(\Omega_g^d\right) = \begin{pmatrix} \mathbf{L}\left(\Omega_{g-1}^d\right) + (d-1)\mathbf{I} & -\mathbf{I} & -\mathbf{I} & \cdots & -\mathbf{I} \\ -\mathbf{I} & (d-1)\mathbf{I} & -\mathbf{I} & \cdots & -\mathbf{I} \\ -\mathbf{I} & -\mathbf{I} & (d-1)\mathbf{I} & \cdots & -\mathbf{I} \\ \vdots & \vdots & \vdots & \ddots & \vdots \\ -\mathbf{I} & -\mathbf{I} & -\mathbf{I} & \cdots & (d-1)\mathbf{I} \end{pmatrix}_{d\times d} \tag{27}$$

The characteristic polynomial of the $\mathbf{L}\left(\Omega_g^d\right)$ is determined as:

$$P_g^d(\lambda) = \det\left(\lambda\mathbf{I} - \mathbf{L}\left(\Omega_g^d\right)\right). \tag{28}$$

The matrix $\lambda\mathbf{I} - \mathbf{L}\left(\Omega_g^d\right)$ can be rewritten as:

$$\lambda\mathbf{I} - \mathbf{L}\left(\Omega_g^d\right) = \mathrm{diag}\left((\lambda-d)\mathbf{I} - \mathbf{L}\left(\Omega_{g-1}^d\right), (\lambda-d)\mathbf{I}, \ldots, (\lambda-d)\mathbf{I}\right)_{d\times d} + \begin{pmatrix} \mathbf{I} \\ \vdots \\ \mathbf{I} \end{pmatrix}_{d\times 1} (\mathbf{I}, \ldots, \mathbf{I})_{1\times d}. \tag{29}$$

Now, using the matrix determinant lemma, see e.g. Ref. 44

$$\det(\mathbf{M} + \mathbf{U}\mathbf{V}^{\mathrm{T}}) = \det(\mathbf{M})\det(\mathbf{I} + \mathbf{V}^{\mathrm{T}}\mathbf{M}^{-1}\mathbf{U}), \tag{30}$$

we obtain

$$\begin{aligned}&\det\left(\lambda\mathbf{I}-\mathbf{L}\left(\Omega_g^d\right)\right)\\&=\det\left((\lambda-d)\mathbf{I}-\mathbf{L}\left(\Omega_{g-1}^d\right)\right)[\det((\lambda-d)\mathbf{I})]^{d-1}\det\left(\mathbf{I}+\left((\lambda-d)\mathbf{I}-\mathbf{L}\left(\Omega_{g-1}^d\right)\right)^{-1}+\frac{d-1}{\lambda-d}\mathbf{I}\right)\\&=\det\left(\mathbf{I}-\frac{d-1}{\lambda-d}\mathbf{L}\left(\Omega_{g-1}^d\right)+(\lambda-1)\mathbf{I}\right)[\det((\lambda-d)\mathbf{I})]^{d-1}\\&=\det((\lambda-1)\mathbf{I})[\det((\lambda-d)\mathbf{I})]^{d-2}\det\left[\frac{\lambda(\lambda-d)}{(\lambda-1)}\mathbf{I}-\mathbf{L}\left(\Omega_{g-1}^d\right)\right].\end{aligned}\tag{31}$$

Thus,

$$P_g^d(\lambda)=(\lambda-1)^{d^{g-1}}(\lambda-d)^{(d-2)d^{g-1}}P_{g-1}^d(\varphi_d(\lambda)),\tag{32}$$

where

$$\varphi_d(\lambda)=\lambda(\lambda-d)/(\lambda-1).\tag{33}$$

Laplacian Eigenvectors of Ω_g^d. Analogous to the eigenvalues, the eigenvectors of $\mathbf{L}\left(\Omega_g^d\right)$ can also be derived directly from those of $\mathbf{L}\left(\Omega_{g-1}^d\right)$. Assume that λ is an eigenvalue of Laplacian matrix for Ω_g^d, the corresponding eigenvector of which is $v\in\mathbf{R}^{d^g}$, where $\mathbf{R}^{d^g}$ is the d^g-dimensional vector space. Then the eigenvector v can be determined by solving equation $\left(\lambda\mathbf{I}_g-\mathbf{L}\left(\Omega_g^d\right)\right)v=0$. We distinguish two cases: $\lambda\in\Lambda_g^{(1)}$ and $\lambda\in\Lambda_g^{(2)}$, which will be separately treated as follows.

For the case of $\lambda\in\Lambda_g^{(1)}$, in which all $\lambda=d$, equation $\left(\lambda\mathbf{I}_g-\mathbf{L}\left(\Omega_g^d\right)\right)v=0$ becomes

$$\begin{pmatrix}\mathbf{I}_{g-1}-\mathbf{L}\left(\Omega_{g-1}^d\right) & \mathbf{I}_{g-1} & \mathbf{I}_{g-1} & \cdots & \mathbf{I}_{g-1}\\ \mathbf{I}_{g-1} & \mathbf{I}_{g-1} & \mathbf{I}_{g-1} & \cdots & \mathbf{I}_{g-1}\\ \mathbf{I}_{g-1} & \mathbf{I}_{g-1} & \mathbf{I}_{g-1} & \cdots & \mathbf{I}_{g-1}\\ \vdots & \vdots & \vdots & \ddots & \vdots\\ \mathbf{I}_{g-1} & \mathbf{I}_{g-1} & \mathbf{I}_{g-1} & \cdots & \mathbf{I}_{g-1}\end{pmatrix}\begin{pmatrix}v_1\\v_2\\v_3\\\vdots\\v_d\end{pmatrix}=0,\tag{34}$$

where vector $v_i(1\le i\le d)$ are components of v. Equation (34) leads to the following equations:

$$\begin{cases}v_1+v_2+v_3+\ldots+v_d=\mathbf{L}\left(\Omega_{g-1}^d\right)v_1,\\v_1+v_2+v_3+\ldots+v_d=0.\end{cases}\tag{35}$$

Then we know that v_1 is the eigenvector corresponding to the eigenvalue 0 in $\mathbf{L}\left(\Omega_{g-1}^d\right)$, that is, $v_1=(1,\,1,\,\cdots,\,1)^T$. Let $v_i=(v_{i,1},v_{i,2},\ldots,v_{i,d^g})^T$, then, Eq. (35) is equivalent to the following equations:

$$\sum_{i=2}^{d}v_{i,j}=-v_{1,j},(j=1,\,2,\,\cdots,\,d^{g-1}).\tag{36}$$

The set of all solutions to any of the above equations consists of vectors of the following form

$$\begin{pmatrix}v_{2,j}\\v_{3,j}\\v_{4,j}\\\vdots\\v_{n,j}\end{pmatrix}=\begin{pmatrix}-v_{1,j}\\0\\0\\\vdots\\0\end{pmatrix}+k_{1,j}\begin{pmatrix}-1\\1\\0\\\vdots\\0\end{pmatrix}+k_{2,j}\begin{pmatrix}-1\\0\\1\\\vdots\\0\end{pmatrix}+\cdots+k_{d-2,j}\begin{pmatrix}-1\\0\\0\\\vdots\\1\end{pmatrix},\tag{37}$$

where $k_{1,j},k_{2,j},\ldots,k_{d-2,j}$ are arbitrary real numbers. In Eq. (37), the solutions for all the vectors $v_i(2\le i\le d)$ can be rewritten as

$$\begin{pmatrix}v_2^T\\v_3^T\\v_4^T\\\vdots\\v_n^T\end{pmatrix}=\begin{pmatrix}-v_1^T\\0\\0\\\vdots\\0\end{pmatrix}+\begin{pmatrix}-1 & -1 & \cdots & -1\\1 & 0 & \cdots & 0\\0 & 1 & \cdots & 0\\\vdots & \vdots & & \vdots\\0 & 0 & \cdots & 1\end{pmatrix}\begin{pmatrix}k_{1,1} & k_{1,2} & k_{1,3} & \cdots & k_{1,n^{t-1}}\\k_{2,1} & k_{2,2} & k_{2,3} & \cdots & k_{2,n^{t-1}}\\k_{3,1} & k_{3,2} & k_{3,3} & \cdots & k_{3,n^{t-1}}\\\vdots & \vdots & \vdots & & \vdots\\k_{n-2,1} & k_{n-2,2} & k_{n-2,3} & \cdots & k_{n-2,n^{t-1}}\end{pmatrix},\tag{38}$$

where $k_{i,j}(1\le i\le d-2;1\le j\le d^{g-1})$ are arbitrary real numbers. Using Eq. (38), we can obtain the eigenvector v associated with the eigenvalue d. Furthermore, we can easily check that the dimension of the eigenspace of matrix $\mathbf{L}\left(\Omega_g^d\right)$ corresponding to eigenvalue d is $(d-2)d^{g-1}$.

We proceed to address the case of $\lambda\in\Lambda_g^{(2)}$. For this case, equation $\left(\lambda\mathbf{I}_g-\mathbf{L}\left(\Omega_g^d\right)\right)v=0$ can be rewritten as

$$\begin{pmatrix}\left(\lambda\left(\Omega_g^d\right)-d+1\right)\mathbf{I}_{g-1}-\mathbf{L}\left(\Omega_{g-1}^d\right) & \mathbf{I}_{g-1} & \cdots & \mathbf{I}_{g-1}\\ \mathbf{I}_{g-1} & \left(\lambda\left(\Omega_g^d\right)-d+1\right)\mathbf{I}_{g-1} & \cdots & \mathbf{I}_{g-1}\\ \vdots & \vdots & & \vdots\\ \mathbf{I}_{g-1} & \mathbf{I}_{g-1} & \cdots & \left(\lambda\left(\Omega_g^d\right)-d+1\right)\mathbf{I}_{g-1}\end{pmatrix}\begin{pmatrix}v_1\\v_2\\\vdots\\v_n\end{pmatrix}=0,\tag{39}$$

where vector $v_i(1\le i\le d)$ are components of v. Eq (39) leads to the following equations:

$$\begin{cases}\left(\left(\lambda\left(\Omega_g^d\right)-d+1\right)\mathbf{I}_{g-1}-\mathbf{L}\left(\Omega_{g-1}^d\right)\right)v_1+v_2+v_3+\cdots+v_n=0,\\v_1+\left(\lambda\left(\Omega_g^d\right)-d+1\right)v_2+v_3+\cdots+v_n=0,\\v_1+v_2+\left(\lambda\left(\Omega_g^d\right)-d+1\right)v_3+\cdots+v_n=0,\\\vdots\\v_1+v_2+v_3+\cdots+\left(\lambda\left(\Omega_g^d\right)-d+1\right)v_n=0.\end{cases}\tag{40}$$

Resolving Eq. (40) yields

$$\begin{cases}\left(\frac{\lambda\left(\Omega_g^d\right)\left(\lambda\left(\Omega_g^d\right)-d\right)}{\lambda\left(\Omega_g^d\right)-1}\mathbf{I}_{g-1}-\mathbf{L}\left(\Omega_{g-1}^d\right)\right)v_1=0,\\v_2=v_3=\cdots=v_n=-\frac{1}{\lambda\left(\Omega_g^d\right)-1}v_1.\end{cases}\tag{41}$$

As demonstrated in the first subsection of Methods, if λ is an eigenvalue of $\lambda\left(\Omega_g^d\right)$, then $\varphi_d(\lambda)=\frac{\lambda(\lambda-d)}{\lambda-1}$ is an eigenvalue of $\lambda\left(\Omega_{g-1}^d\right)$. When $i\le d^{g-1}$, we have $\frac{\lambda\left(\Omega_g^d\right)\left(\lambda\left(\Omega_g^d\right)-d\right)}{\lambda\left(\Omega_g^d\right)-1}=\lambda_i\left(\Omega_{g-1}^d\right)$, while in the situation $d^{g-1}<i\le 2d^{g-1}$, $\frac{\lambda\left(\Omega_g^d\right)\left(\lambda\left(\Omega_g^d\right)-d\right)}{\lambda\left(\Omega_g^d\right)-1}=\lambda_{i-d^{g-1}}\left(\Omega_{g-1}^d\right)$. From Eq. (41), vector v_1 is the eigenvector of $\mathbf{L}\left(\Omega_{g-1}^d\right)$ corresponding to the eigenvalue $\lambda_i\left(\Omega_{g-1}^d\right)$. Applying the v_1 into Eq. (41), we will get all of the $v_i(2\le i\le d)$ and finally the eigenvector of $\mathbf{L}\left(\Omega_g^d\right)$ corresponding to $\lambda_i\left(\Omega_g^d\right)$. In this way, we have completely determined all eigenvalues and their corresponding eigenvectors of $\mathbf{L}\left(\Omega_g^d\right)$.

1. Newman, M., Barabási, A. L. & Watts, D. J. (Eds.) *The Structure and Dynamics of Networks* (Princeton University Press, 2006).
2. Grosberg, A. Yu. & Khokhlov, A. R. *Statistical Physics of Macromolecules* (AIP Press, New York, 1994).
3. Gurtovenko, A. A. & Blumen, A. Generalized Gaussian Structures: Models for Polymer Systems with Complex Topologies. *Adv. Polym. Sci.* **182**, 171–277 (2005).
4. Sommer, J. U. & Blumen, A. On the statistics of generalized Gaussian structures: Collapse and random external fields. *J. Phys. A* **28**, 6669–6674 (1995).
5. Schiessel, H. Unfold dynamics of generalized Gaussian structures. *Phys. Rev. E* **57**, 5775–5781 (1998).
6. Blumen, A., Volta, A., Jurjiu, A. & Koslowski, Th. Monitoring energy transfer in hyperbranched macromolecules through fluorescence depolarization. *J. Lumin.* **111**, 327–334 (2005).
7. Blumen, A., Volta, A., Jurjiu, A. & Koslowski, Th. Energy transfer and trapping in regular hyperbranched macromolecules. *Physica A* **356**, 12–18 (2005).
8. Galiceanu, M. & Blumen, A. Spectra of Husimi cacti Exact results and applications. *J. Chem. Phys.* **127**, 134904 (2007).
9. Zhang, Z. Z., Wu, B., Zhang, H. J., Zhou, S. G., Guan, J. H. &Wang, Z. G. Determining global mean-first-passage time of random walks on Vicsek fractals using eigenvalues of Laplacian matrices. *Phys. Rev. E* **81**, 031118 (2010).
10. Guérin, T., Bénichou, O. & Voituriez, R. Non-Markovian polymer reaction kinetics. *Nat. Chem.* **4**, 568–573 (2012).
11. Bénichou, O. & Voituriez, R. From first-passage times of random walks in confinement to geometry-controlled kinetics. *Phys. Rep.* **539**, 225–284 (2014).
12. Dobrin, R. & Duxbury, P. M. Minimum Spanning Trees on Random Networks. *Phys. Rev. Lett.* **86**, 5076–5079 (2001).
13. Wu, F. Y. Theory of resistor networks: the two-point resistance. *J. Phys. A: Math. Gen.* **37**, 6653–6673 (2004).
14. Newman, M. E. J. Finding community structure in networks using the eigenvectors of matrices. *Phys. Rev. E* **74**, 036104 (2006).
15. Cosenza, M. G. & Kapral, R. Coupled maps on fractal lattices. *Phys. Rev. A* **46**, 1850–1858 (1992).

16. Marini, U., Marconi, B. & Petri, A. Time dependent Ginzburg - Landau model in the absence of translational invariance. Non-conserved order parameter domain growth. *J. Phys. A* **30**, 1069–1088 (1997).
17. Cai, C. & Chen, Z. Y. Rouse dynamics of a dendrimer model in the Theta condition. *Macromolecules* **30**, 5104–5117 (1997).
18. Jayanthi, C. S., Wu, S. Y. & Cocks, J. Real space Greens function approach to vibrational dynamics of a Vicsek fractal. *Phys. Rev. Lett.* **69**, 1955–1958 (1992).
19. Jayanthi, C. S. & Wu, S. Y. Dynamics of a Vicsek fractal: The boundary effect and the interplay among the local symmetry, the self-similarity, and the structure of the fractal. *Phys. Rev. B* **50**, 897–906 (1994).
20. Sokolov, I. M., Klafter, J. & Blumen, A. Fractional Kinetics. *Phys. Today* **55**, 48–54 (2002).
21. Newkome, G. R. & Moorefield, C. N. From 1 → 3 dendritic designs to fractal supramacromolecular constructs: understanding the pathway to the Sierpinski gasket. *Chem. Soc. Rev.* DOI:10.1039/c4cs00234b (2015). (in press)
22. Jespersen, S., Sokolov, I. M. & Blumen, A. Small-world Rouse networks as models of cross-linked polymers. *J. Chem. Phys.* **113**, 7652–7655 (2000).
23. Zhang, Z. Z., Li, X. T., Lin, Y. & Chen, G. R. Random walks in small-world exponential treelike networks. *J. Stat. Mech-Theory E.* P08013 (2011).
24. Gurtovenko, A. A. & Blumen, A. Relaxation of disordered polymer networks: Regular lattice made up of small-world Rouse networks. *J. Chem. Phys.* **115**, 4924–4929 (2001).
25. Jespersen, S., Sokolov, I. M. & Blumen, A. Relaxation properties of small-world networks. *Phys. Rev. E* **62**, 4405–4408 (2000).
26. Watts, D. J. & Strogatz, S. H. Collective dynamics of 'small-world' networks. *Nature* **393**, 440–442 (1998).
27. Amaral, L. A. N., Scala, A., Barthélémy, M. & Stanley, H. E. Classes of small-world networks. *Proc. Natl. Acad. Sci. U.S.A.* **97**, 11149–11152 (2000).
28. Hillery, M., Reitzner, D. & Bužek, V. Searching via walking: How to find a marked clique of a complete graph using quantum walks. *Phys. Rev. A* **81**, 062324 (2010).
29. Anishchenko, A., Blumen, A. & Mülken, O. Enhancing the spreading of quantum walks on star graphs by additional bonds. *Quantum Inf. Process.* **11**, 1273–1286 (2012).
30. Marti, K. H., Bauer, B., Reiher, M., Troyer, M. & Verstraete, F. Complete-graph tensor network states: a new fermionic wave function ansatz for molecules. *New J. Phys.* **12**, 103008 (2010).
31. Bonneau, J., Anderson, J., Anderson, R. & Stajano, F. Eight Friends Are Enough: Social Graph Approximation via Public Listings. *SNS '09 Proceedings of the Second ACM EuroSys Workshop on Social Network Systems* 13–18 (2009).
32. Lee, H. K., Kim, B. J. & Park, H. Continuity of the explosive percolation transition. *Phys. Rev. E* **84**, 020101 (2011).
33. Wu, S., Zhang, Z. Z. & Chen, G. Random walks on dual Sierpinski gaskets. *Eur. Phys. J. B* **82**, 91–96 (2011).
34. Newman, M. E. J. The structure and function of complex networks. *SIAM Rev.* **45**, 167 (2003).
35. Alexander, S. & Orbach, R. Density of states on fractals: "fractons" *J. Physique Lett.* **43**, L625–L631 (1982).
36. Blumen, A., von Ferber, Ch., Jurjiu, A. & Koslowski, Th. Generalized Vicsek fractals: Regular hyperbranched polymers. *Macromolecules* **37**, 638–650 (2004).
37. Jurjiu, A., Friedrich, Ch. & Blumen, A. Strange kinetics of polymeric networks modelled by finite fractals. *Chem. Phys.* **284**, 221–231 (2002).
38. Blumen, A. & Jurjiu, A. Multifractal spectra and the relaxation of model polymer networks. *J. Chem. Phys.* **116**, 2636–2641 (2002).
39. Biswas, P., Kant, R. & Blumen, A. Polymer dynamics and topology: Extension of stars and dendrimers in external fields. *Macromol. Theory Simul.* **9**, 56–67 (2000).
40. Rouse, P. E. A theory of the linear viscoelastic properties of dilute solutions of coiling polymers. *J. Chem. Phys.* **21**, 1272–1280 (1953).
41. Doi, M. & Edwards, S. F. *The Theory of Polymer Dynamics* (Clarendon, Oxford, 1986).
42. Amblard, F., Maggs, A. C., Yurke, B., Pargellis, A. N. & Leibler, S. Subdiffusion and anomalous local viscoelasticity in actin networks. *Phys. Rev. Lett.* **77**, 4470–4473 (1996).
43. Ferry, J. D. *Viscoelastic Properties of Polymers*, 3rd ed. (Wiley, New York, 1980).
44. Gianessi, F., Pardalos, P. & Rapcsak, T. *Optimization Theory* (Kluwer academic publishers, 2001).

Acknowledgments

This work was supported by the National Natural Science Foundation of China under Grant No. 11275049. M.D. acknowledges DFG through Grant No. Bl 142/11-1 and through IRTG "Soft Matter Science" (GRK 1642/1).

Author contributions

H.L., M.D. and Z.Z.Z. designed the research. H.L. and Y.Q. performed the research. H.L., M.D. and Z.Z.Z. wrote the manuscript.

Additional information

Competing financial interests: The authors declare no competing financial interests.

How to cite this article: Liu, H., Dolgushev, M., Qi, Y. & Zhang, Z. Laplacian spectra of a class of small-world networks and their applications. *Sci. Rep.* **5**, 9024; DOI:10.1038/srep09024 (2015).